Condensation vs. phase-ordering in the dynamics of first order transitions

C. Castellano¹, F. Corberi^{1,2} and M. Zannetti¹

1 Istituto Nazionale di Fisica della Materia, Unità di Salerno and Dipartimento di Fisica, Università di Salerno, 84081

Baronissi (Salerno), Italy

2 Dipartimento di Scienze Fisiche, Università di Napoli, Mostra d'Oltremare, Padiglione 19, 80125 Napoli, Italy

The origin of the non commutativity of the limits $t \to \infty$ and $N \to \infty$ in the dynamics of first order transitions is investigated. In the large-N model, i.e. $N \to \infty$ taken first, the low temperature phase is characterized by condensation of the large wave length fluctuations rather than by genuine phase-ordering as when $t \to \infty$ is taken first. A detailed study of the scaling properties of the structure factor in the large-N model is carried out for quenches above, at and below T_c . Preasymptotic scaling is found and crossover phenomena are related to the existence of components in the order parameter with different scaling properties. Implications for phase-ordering in realistic systems are discussed.

PACS: 05.70.Fh, 64.60.Cn, 64.60.My, 64.75.+g e-mail: castellano@na.infn.it, corberi@na.infn.it, zannetti@na.infn.it

I. INTRODUCTION

The large time behavior of a system quenched at or below the critical point is characterized by scale invariance [1]. For the equal time structure factor one has

$$C(\vec{k},t) = L^{\alpha}(t)F(kL(t)) \tag{1}$$

where

$$L(t) \sim t^{\frac{1}{z}} \tag{2}$$

is the characteristic length growing with time according to a power law and F(x) is the scaling function. The physics behind (1) is quite simple and is basically due to the degeneracy of the low temperature state. After the quench an exponentially fast process takes place leading to local equilibrium. If multiple choice is available, correlated regions of the possible low temperature phases are formed. From that point onward equilibration proceeds through the coarsening of these correlated regions, whose characteristic size L(t) grows according to (2). The difference between quenches to T_c and below T_c is that in the first case the correlated regions are fractal (Appendix I), while in the second one are compact. Apart from this, in both cases the equilibration process becomes slow (if the system is infinite, equilibrium is never reached) and after domains of the ordered phases have formed, scaling behavior occurs since the residual time dependence is confined in the typical size L(t) of the correlated regions.

The whole time evolution can be divided into a preasymptotic and an asymptotic regime, with a smooth transition between the two. The asymptotic regime displays universality and it is controlled by a fixed point structure. The universality classes are determined by features like the presence or absence of a conservation law, the number N of components of the order parameter, the dimensionality d of space and the final temperature T_F of the quench. More precisely, on the temperature axis there is an unstable fixed point at the critical temperature T_c and an attractive fixed point at $T_F = 0$. For the exponent α one has

$$\alpha = \begin{cases} 2 - \eta, \text{ for } T_F = T_c \\ d, \text{ for } T_F < T_c \end{cases}$$
(3)

where η is the usual exponent of the static critical phenomena. The exponent z coincides with the exponent of the dynamical critical phenomena for $T_F = T_c$. Instead, for any final temperature below T_c , z = 2 for non conserved order parameter (NCOP), while for conserved order parameter (COP) z = 3 when N = 1 and z = 4 when N > 1. The scaling function F(x) also displays universal features and it is sensitive to the space dimensionality through the presence (N < d) or absence (N > d) of localized topological defects. By contrast, in the preasymptotic regime the evolution of the system is not universal, as it depends on the initial conditions of the quench and on the actual value of the final temperature.

A complete theory of the process then should derive the scaling behavior from the basic equation of motion for the order parameter and should be able to describe how the relatively simple universal asymptotic regime emerges out of the complexity of the preasymptotic regime. Ideally, one would like to have a manageable reference theory which

accounts, at least qualitatively, for the basic features of the process and a systematic procedure for the computation of the corrections [2]. A scheme of this type is available for quenches to T_c , where, despite the difficulty due to the lack of time translational invariance, the field theoretical machinery developed for critical phenomena is to a large extent applicable [3]. Instead, for quenches below T_c the present status of theoretical understanding is far from this standard. What we have in this case is the linear theory [4] for the very early stage of the process, which applies only when initial conditions are so small that it is actually justified to employ a linear approximation, and *ad hoc* late stage theories [5]. Although these late stage theories have had much success in the computation of the scaling functions, yet are based on uncontrolled approximations. Furthermore, the late stage theories do not connect to the early stage theory, if this is available at all. So, there is no theoretical understanding of the complex phenomenology arising at the breakdown of the early stage theory and leading to the onset of scaling [6]. Proposals for the systematic improvement of the late stage theory have been put forward [7] but, as of now, a first principles theory of phase-ordering processes is out of reach.

In this theoretical landscape a special position is occupied by the 1/N-expansion. As applied to critical phenomena this technique provides a very clear instance of what is to be understood for a systematic theory: there is a lowest order analytically tractable approximation (the large-N model) which captures the basic physics and there is an expansion parameter (1/N) which allows for the systematic computation of the corrections. The scheme applies succesfully also to quenches to the critical point [3] and, at first sight, it would seem to be applicable as well to the phase-ordering processes. Indeed, in the large-N model one can solve exactly [8] for the structure factor and one finds that the standard scaling form (1) is obeyed for large time with NCOP [9]. In particular one finds z = 2, and α is given by (3) with $\eta = 0$. The scaling functions can also be found explicitly [10]. It is to be stressed that in the solution of the model with $N = \infty$ there are no *ad hoc* hypotheses and the above outlined picture of the asymptotic behavior with scaling, universality and temperature fixed points is derived from the solution of the equation of motion.

However, when the model is solved with COP [8,10], although the form (1) is obeyed with $\alpha = 2$ and z = 4 for $T_F = T_c$, for the quenches to $T_F < T_c$ the more general multiscaling form

$$C(\vec{k},t) \sim \left[L(k_m L)^{\frac{2-d}{d}}\right]^{\alpha(x)} F(x) \tag{4}$$

is found, where $L(t) \sim t^{1/4}$, $k_m(t)$ is the peak wave vector and $x = k/k_m$. The exponent $\alpha(x)$ is given by

$$\alpha(x) = q + \varrho\varphi(x) \tag{5}$$

with

$$q = \begin{cases} 2, \text{ for } 0 < T_F < T_c \\ 0, \text{ for } T_F = 0 \end{cases}$$
(6)

$$\varrho = \begin{cases} d-2, \text{ for } 0 < T_F < T_c \\ d, \text{ for } T_F = 0. \end{cases}$$
(7)

Furthermore, when $0 < T_F < T_c$ the function $\varphi(x)$ in (5) is given by

$$\varphi(x) = \begin{cases} \psi(x), & \text{for } x < x^* \\ 0, & \text{for } x > x^* \end{cases}$$
(8)

with $x^* = \sqrt{2}$ and

$$\psi(x) = 1 - (1 - x^2)^2 \tag{9}$$

while $\varphi(x) = \psi(x)$ for all values of x when $T_F = 0$. Finally,

$$F(x) = \begin{cases} \frac{T_F}{x^2}, & \text{for } 0 < T_F < T_c \\ 1, & \text{for } T_F = 0. \end{cases}$$
(10)

Leaving aside for the moment the apparent formal complication of (4-10), the important feature which is immediately evident is that, contrary to (3), now there are three distinct asymptotic behaviors for $T_F = T_c$, for $0 < T_F < T_c$ and for $T_F = 0$. For $T_F = T_c$ the structure factor obeys standard scaling with $\alpha = 2$ as in the NCOP case. Instead for $T_F < T_c$ the exponent α depends on x (Fig. 1) and the scaling form (4) involves two lengths, $k_m^{-1}(t)$ and L(t), which differ by a logarithmic factor [8]

$$(k_m L)^4 = \log L^d + (2 - d) \log(k_m L).$$
(11)

The functional form of $\alpha(x)$ is different for $0 < T_F < T_c$ and for $T_F = 0$. This means that $T_F = T_c$ and $T_F = 0$ are both unstable fixed points and in between there is a new line of fixed points for $0 < T_F < T_c$. The temperature below the critical point is no more an irrelevant variable.

If the 1/N expansion were a good systematic theory, the 1/N corrections ought to produce only minor quantitative changes on the picture outlined above. However, this expectation has not been fulfilled by the work of Bray and Humayun (BH) [11], who found that for quenches to $T_F = 0$ and COP standard scaling of the form (1) is restored in systems with any finite value of N. The same result is very likely to apply also to the quenches to $0 < T_F < T_c$. Therefore, the main qualitative features emerging in lowest order, like the multiscaling behavior and the relevance of the temperature fluctuations, are expected to be a peculiarity of the case with N strictly infinite, disappearing as soon as higher order corrections are taken into account. In other words, the limits $N \to \infty$ and $t \to \infty$ do not commute for quenches to $T_F < T_c$. In this paper we explore in some detail this phenomenon and we clarify what dynamical process is really described when the $N \to \infty$ limit is taken first. This helps to understand what correct use is to be made of the large-N model in this area of non equilibrium statistical mechanics.

The gross features of what goes on in the quenches below T_c can be described with the help of Figure 2. The phase-ordering process of a system with finite N is represented by path I connecting the disordered states A to the ordered states B. These latter states are mixtures of broken symmetry states. If, after equilibrium has been established, the $N \to \infty$ limit is taken as depicted by path II, the system is brought into a state D which is the mixture of the $N \to \infty$ limits of each one of the broken symmetry states. If, instead, the $N \to \infty$ limit is taken before the quench, the process starts from a disordered state C of the system with infinitely many components and the ensuing dynamical process does not connect C to D along path III. As a matter of fact, the process depicted by III does not exist. Rather, the dynamical evolution follows path IV leading to low temperature states E which are quite distinct from D. In other words, the system with $N = \infty$ supports two different low temperature phases, whose realization depends on the order of the limits $t \to \infty$ and $N \to \infty$. The distinction between these two phases is reminiscent of the difference between the zero field low temperature states in the spherical model [12] and in the mean spherical model [13]. In particular, states E are very similar to the low temperature states in the ideal Bose gas, as it will be clarified in the next section. The point to be stressed here is that in the static 1/N expansion states A and B are reached, respectively, from states C and D, while 1/N corrections over states E are not informative on states B. This clarifies why the 1/N expansion can be used for quenches to T_c , but not below T_c , as an approximation for processes with finite N.

What, then, is the use of the large-N model for growth kinetics. There is an obvious intrinsic interest, once it is clear that although not describing a phase-ordering process of the usual type, yet the model is well defined and describes the relaxation across a phase transition. The growth process generated in the time evolution can be studied in detail and produces non trivial behavior. The outcome is quite interesting since, by modulating the initial noise and the final temperature, remarkable crossover phenomena are obtained. Here is where the model gives information also on systems with finite N, even if it is not perturbatively close to the phase-ordering processes. In fact, the phenomenology of the structure factor exhibits features which are also found in the preasymptotic behavior of systems with finite N [14,15]. Therefore, through the large-N model insight can be gained into the very complex time regime preceding the onset of scaling in realistic systems.

The paper is organized as follows. In Section II the model is introduced, the non commutativity of the $t \to \infty$, $N \to \infty$ limits is clarified and the nature of the low temperature phases in the large-N model is investigated. In Section III the numerical solution for the structure factor is presented and crossovers between different scaling behaviors are analyzed by means of the multiscaling analysis. Conclusions are presented in Section IV.

II. THE LOW TEMPERATURE PHASES

In the following we consider the relaxation dynamics of a system with an N-component order parameter $\phi(\vec{x}) = (\phi_1(\vec{x}), \dots, \phi_N(\vec{x}))$ which is initially prepared in a high temperature disordered state and it is suddenly quenched to a lower temperature. The evolution of the order parameter is governed by the time-dependent Ginzburg-Landau model

$$\frac{\partial \vec{\phi}(\vec{x},t)}{\partial t} = -(i\nabla)^p \frac{\partial \mathcal{H}[\vec{\phi},N]}{\partial \vec{\phi}(\vec{x})} + \vec{\eta}(\vec{x},t)$$
(12)

where p = 0 for NCOP, p = 2 for COP, and $\vec{\eta}(\vec{x}, t)$ is the gaussian white noise with expectations

$$\begin{cases} < \vec{\eta}(\vec{x},t) > = 0 \\ < \eta_{\alpha}(\vec{x},t)\eta_{\beta}(\vec{x}',t') > = 2T_F(i\nabla)^p \delta_{\alpha\beta} \delta(\vec{x}-\vec{x}')\delta(t-t'). \end{cases}$$
(13)

The free energy functional is of the form

$$\mathcal{H}[\vec{\phi}, N] = \int_{V} d^{d}x \left[\frac{1}{2} (\nabla \vec{\phi})^{2} + \frac{r}{2} \vec{\phi}^{2} + \frac{g}{4N} (\vec{\phi}^{2})^{2} \right]$$
(14)

where V is the volume of the system and r < 0, g > 0. The order parameter probability distribution in the initial state can be taken of the form

$$P_0[\vec{\phi}, N] = \frac{1}{Z_0} \exp\left\{-\frac{1}{2\Delta} \int d^d x \vec{\phi}^2(\vec{x})\right\}$$
(15)

describing the absence of correlations at high temperature

$$\langle \phi_{\alpha}(\vec{x},0)\phi_{\beta}(\vec{x}',0)\rangle = \Delta\delta_{\alpha\beta}\delta(\vec{x}-\vec{x}').$$
(16)

As mentioned in the Introduction, if one wants to consider the $N \to \infty$ limit, in order to determine the nature of the final equilibrium state attention must be payed to the order in which the $N \to \infty$ and $t \to \infty$ limits are taken. Let us consider first the sequence $\lim_{N\to\infty} \lim_{t\to\infty}$. Keeping N finite, the equation of motion (12) induces the time evolution of the probability distribution from the initial form (15) toward the Gibbs state

$$P[\vec{\phi}, t, N] \longrightarrow P_{eq}[\vec{\phi}, N] = \frac{1}{Z} \exp\left\{-\frac{1}{T_F} \mathcal{H}[\vec{\phi}, N]\right\}.$$
(17)

In the infinite volume limit $P_{eq}[\vec{\phi}, N]$ describes a disordered pure state if T_F is above T_c and the O(N) symmetrical mixture of the broken symmetry states if T_F is below T_c . If we now take the $N \to \infty$ limit (path of type II in Fig. 1), for $T_F \ge T_c$ we obtain the pure phase C

$$P_{eq}[\vec{\phi},\infty] = \frac{1}{Z} \exp\left\{-\frac{1}{2T_F} \sum_{\vec{k}} (k^2 + r + gS)\vec{\phi}(\vec{k}) \cdot \vec{\phi}(-\vec{k})\right\}$$
(18)

where S is given by the self-consistency condition

$$S = \frac{1}{V} \sum_{\vec{k}} \langle \phi_{\beta}(\vec{k})\phi_{\beta}(-\vec{k}) \rangle$$
(19)

and β denotes the generic component. Below T_c , denoting by \vec{m} the expectation value of $\vec{\phi}(\vec{x})$ in the broken symmetry state, the $N \to \infty$ limit D of the mixture is obtained

$$P_{eq}[\vec{\phi},\infty] = \int d\vec{m}\rho(\vec{m})\mu[\vec{\phi} \mid \vec{m}]$$
⁽²⁰⁾

where $\rho(\vec{m})$ is the uniform probability density over the sphere of radius *m* and the pure state $\mu[\vec{\phi} \mid \vec{m}]$ is given by

$$\mu[\vec{\phi} \mid \vec{m}] = \delta[(\vec{\phi} - \vec{m}) \cdot \hat{m}] \frac{1}{Z} \exp\left\{-\frac{1}{2T_F} \sum_{\vec{k}} (k^2 + r + gm^2 + gS_{\perp}) \vec{\phi}_{\perp}(\vec{k}) \cdot \vec{\phi}_{\perp}(-\vec{k})\right\}$$
(21)

where $\vec{\phi}_{\perp} = \vec{\phi} - (\vec{\phi} \cdot \hat{m})\hat{m}$. The quantities S_{\perp} and m are determined by the self-consistency relations

$$S_{\perp} = \frac{1}{V} \sum_{\vec{k}} \langle \phi_{\perp\beta}(\vec{k}) \phi_{\perp\beta}(-\vec{k}) \rangle$$
(22)

$$r + g(m^2 + S_\perp) = 0. (23)$$

In the end, computing averages with the weight functions (18) (20), we find the well known result of the large-N model

$$\langle \phi_{\beta}(\vec{k})\phi_{\beta}(-\vec{k}) \rangle = \begin{cases} \frac{T_F}{k^2 + r + gS}, & \text{for } T_F \ge T_c \\ \frac{T_F}{k^2} + m^2 \delta(\vec{k}), & \text{for } T_F < T_c \end{cases}$$
(24)

for the equilibrium structure factor in states C and D. The average value of the order parameter is given by

$$m^2 = -\frac{r}{g} \left(\frac{T_c - T_F}{T_c} \right) \tag{25}$$

with

$$T_c = -\frac{r(d-2)}{gK_d\Lambda^{d-2}} \tag{26}$$

where Λ is a wave vector cutoff and $K_d = [2^{d-1}\pi^{d/2}\Gamma(d/2)]^{-1}$. The $\delta(\vec{k})$ term appearing in (24), below T_c , is the Bragg peak due to ordering in the low temperature phase D.

Let us now consider the limits in the opposite order. Taking the $N \to \infty$ limit at the outset amounts to take the limit on the equation of motion (12) which becomes effectively linearized

$$\frac{\partial \phi_{\beta}(\vec{k},t)}{\partial t} = -k^{p}[k^{2} + R(t)]\phi_{\beta}(\vec{k},t) + \vec{\eta}_{\beta}(\vec{k},t)$$
(27)

with

$$R(t) = r + gS(t) \tag{28}$$

and

$$S(t) = \frac{1}{V} \sum_{\vec{k}} \langle \phi_{\beta}(\vec{k}, t) \phi_{\beta}(-\vec{k}, t) \rangle .$$
⁽²⁹⁾

Due to the linearity of Eq. (27), the time dependent probability distribution is gaussian

$$P[\vec{\phi}, t, \infty] = \frac{1}{Z(t)} \exp\left\{-\frac{1}{2} \sum_{\vec{k}} C^{-1}(\vec{k}, t) \vec{\phi}(\vec{k}) \cdot \vec{\phi}(-\vec{k})\right\}$$
(30)

with

$$C(\vec{k},t) = \langle \phi_{\beta}(\vec{k},t)\phi_{\beta}(-\vec{k},t) \rangle .$$
(31)

Taking next the $t \to \infty$ limit

$$P[\vec{\phi}, t, \infty] \to Q_{eq}[\vec{\phi}, \infty] = \frac{1}{Z} \exp\left\{-\frac{1}{2} \sum_{\vec{k}} C_{eq}^{-1}(\vec{k}) \vec{\phi}(\vec{k}) \cdot \vec{\phi}(-\vec{k})\right\}$$
(32)

we obtain a gaussian state for any final temperature and it is legitimate to ask whether still there is a phase transition. From (27) it is straightforward to obtain [10] the equation of motion for the structure factor

$$\frac{\partial C(\vec{k},t)}{\partial t} = -2k^p [k^2 + R(t)]C(\vec{k},t) + 2k^p T_F$$
(33)

which, after equilibration is reached, yields

$$C_{eq}(\vec{k}) = \frac{T_F}{k^2 + \xi^{-2}} \tag{34}$$

with NCOP and

$$C_{eq}(\vec{k}) = \begin{cases} C(\vec{k}=0, t=0), & \text{for } \vec{k}=0\\ \frac{T_F}{k^2 + \xi^{-2}}, & \text{for } \vec{k} \neq 0 \end{cases}$$
(35)

with COP, where $\lim_{t\to\infty} R(t) = \xi^{-2}$ is the inverse square equilibrium correlation length. From (28)

$$\xi^{-2} = r + \frac{gT_F}{V} \sum_{\vec{k}} \frac{1}{k^2 + \xi^{-2}}$$
(36)

where the sum extends over all values of \vec{k} for NCOP and over $\vec{k} \neq 0$ for COP. We now analyze Eq. (36) in the NCOP case referring to Appendix II for the modifications in the argument required by the conservation law. With V finite the solution of Eq. (36) for ξ is finite for any temperature. As expected, there is no phase transition in a finite volume system. In the infinite volume limit (36) becomes

$$\xi^{-2} = r + gT_F B(\xi^{-2}) + \frac{gT_F}{V\xi^{-2}}$$
(37)

where the function B(x) defined by

$$B(x) = \int \frac{d^d k}{(2\pi)^d} \frac{1}{k^2 + x}$$
(38)

is a monotonously decreasing function of x with a maximum value at $B(0) = K_d \Lambda^{d-2}/(d-2)$. In writing (37) the $\vec{k} = 0$ contribution to the sum (36) has been explicitly separated out. Defining $\gamma^2 = \frac{T_F}{V\xi^{-2}}$ and introducing the temperature $T_c = -\frac{r}{qB(0)}$ which coincides with (26), Eq. (37) can be rewritten as

$$\frac{1}{g}\xi^{-2} = \left[\frac{r}{g}\left(\frac{T_c - T_F}{T_c}\right) + \gamma^2\right] + T_F\left[B(\xi^{-2}) - B(0)\right]$$
(39)

with the solution (Appendix II)

$$\begin{cases} \xi^{-2} > 0, & \gamma^2 = 0, & \text{for } T_F > T_c \\ \xi^{-2} = 0, & \gamma^2 = 0, & \text{for } T_F = T_c \\ \xi^{-2} = 0, & \gamma^2 = -r/g \left(\frac{T_c - T_F}{T_c}\right), & \text{for } T_F < T_c \end{cases}$$
(40)

which shows the existence of the phase transition at T_c . For the structure factor this implies

$$C_{eq}(\vec{k}) = \begin{cases} \frac{T_F}{k^2 + \xi^{-2}} & T_F \ge T_c \\ \frac{T_F}{k^2} + \gamma^2 \delta(\vec{k}) & T_F < T_c \end{cases}$$
(41)

and taking into account the form (40) of γ^2 , (41) is identical to (24). Thus, as far as the structure factor is concerned, the same result is found irrespective of the order of the limits $t \to \infty$ and $N \to \infty$. However, comparing the states, $Q_{eq}[\vec{\phi}, \infty]$ coincides with $P_{eq}[\vec{\phi}, \infty]$ above T_c , but not below where

$$Q_{eq}[\vec{\phi},\infty] = \frac{1}{\sqrt{2\pi\gamma^2 V}} \exp\left\{-\frac{\phi^2(0)}{2\gamma^2 V}\right\} \frac{1}{Z} \exp\left\{-\frac{1}{2}\sum_{\vec{k}\neq 0} C_{eq}^{-1}(\vec{k})\vec{\phi}(\vec{k}) \cdot \vec{\phi}(-\vec{k})\right\}.$$
(42)

This is a state exactly of the same form of the zero field low temperature state in the mean spherical model, while state D is a mixture as in the spherical model [16].

Thus, despite the formal similarity, the Bragg peaks in (24) and (41) have different physical meanings. In the former case, it signals the formation of a mixture of ordered states, while in the latter it is due to the macroscopic growth of the $\vec{k} = 0$ term in the sum (36). What we have here is a low temperature phase obtained by condensation of the fluctuations at $\vec{k} = 0$, as in the ideal Bose gas, with $C_{eq}(\vec{k} = 0)$ playing the role of the zero momentum occupation number.

Finally, notice that with d = 2 the critical temperature (26) vanishes. Hence, all states with $T_F > 0$ are disordered states and the limits $t \to \infty$ and $N \to \infty$ commute for the quenches to any finite final temperature. Conversely, $T_F = 0$ is not a critical temperature, rather it is an ordering temperature. Therefore, the quench to $T_F = 0$ is an ordering process and the limits are not supposed to commute in this case.

III. SCALING BEHAVIORS

In this section we investigate the time evolution of the structure factor by solving numerically the equation of motion (33). It is convenient to comment beforehand on the structure of this solution. Integrating (33) the structure factor can be written as the sum of two contributions

$$C(\vec{k},t) = C_0(\vec{k},t) + C_T(\vec{k},t)$$
(43)

with

$$C_0(\vec{k},t) = \Delta \exp\left\{-2k^p \int_0^t ds \left[k^2 + R(s)\right]\right\}$$
(44)

and

$$C_T(\vec{k},t) = 2T_F k^p \int_0^t dt' \exp\left\{-2k^p \int_{t'}^t ds \left[k^2 + R(s)\right]\right\}.$$
(45)

The asymptotic behavior is analytically accessible and it has been derived in detail in Ref. [10]. For quenches to $T_F \leq T_c$ with NCOP, the large time behavior is given by

$$C_0(\vec{k},t) = \Delta L^\omega f_0(x) \tag{46}$$

$$C_T(\vec{k},t) = T_F L^2 f_T(x) \tag{47}$$

with $L(t) = t^{1/2}$, x = kL and

$$\omega = \begin{cases} 4 - d, \text{ for } T_F = T_c \\ d, \text{ for } T_F < T_c \end{cases}$$
(48)

$$f_0(x) = e^{-x^2} (49)$$

$$f_T(x) = \int_0^1 dy (1-y)^{-\omega/2} e^{-x^2 y}.$$
(50)

Notice that both contributions are in the scaling form (1) with $C_T(\vec{k},t)$ dominating in the quenches to T_c while $C_0(\vec{k},t)$ dominates for $T_F < T_c$. One may go one step further regarding the order parameter as the sum of two contributions $\vec{\phi} = \vec{\sigma} + \vec{\zeta}$ whose correlations account for the two pieces in the structure factor $C_0(\vec{k},t) = <\sigma_\beta\sigma_\beta >$, $C_T(\vec{k},t) = <\zeta_\beta\zeta_\beta >$ and $<\sigma_\beta\zeta_\gamma >= 0$. Therefore, for $T_F < T_c$ a sort of two fluids picture of the quench is obtained, with the condensate $\vec{\sigma}$ and the thermal fluctuations $\vec{\zeta}$ having a distinct individuality due to the different scaling properties. Notice that the irrelevance of the thermal fluctuations is due to $\vec{\sigma}$ dominating $\vec{\zeta}$ and obeying the zero temperature equation of motion.

With COP there is additional structure since the thermal contribution contains itself two different pieces

$$C_T(\vec{k},t) = \begin{cases} C_{<}(\vec{k},t), & \text{for } k < x^* k_m(t) \\ C_{>}(\vec{k},t), & \text{for } k > x^* k_m(t) \end{cases}$$
(51)

with the asymptotic behaviors

$$C_0(\vec{k},t) = \Delta L^{\rho\psi(x)} \tag{52}$$

$$C_{<}(\vec{k},t) = \frac{T_F}{x^2} L^{2+\rho\psi(x)}$$
(53)

$$C_{>}(\vec{k},t) = \frac{T_F}{x^2} L^2 \tag{54}$$

$$\rho = \begin{cases}
0, & \text{for } T_F = T_c \\
d - 2, & \text{for } 0 < T_F < T_c \\
d, & \text{for } T_F = 0.
\end{cases}$$
(55)

For simplicity, in writing (52-54) we have neglected the logarithmic difference between L(t) and $k_m(t)$, putting x = kLand $L(t) = t^{1/4}$. The novelty is in the region $0 < T_F < T_c$, where there is a sharp distinction between what happens for $x < x^*$ and for $x > x^*$. In the first case $C_{\leq}(\vec{k},t)$ dominates over $C_0(\vec{k},t)$, while in the second case $C_{>}(\vec{k},t)$ dominates over $C_0(\vec{k},t)$. Therefore, with COP we are led to regard the order parameter as the sum of three contributions $\vec{\phi} = \vec{\sigma} + \vec{\zeta_{<}} + \vec{\zeta_{>}}$ which, again, are characterized by distinct scaling properties and whose correlations are responsible, respectively, for $C_0(\vec{k},t)$, $C_{<}(\vec{k},t)$ and $C_{>}(\vec{k},t)$. The remarkable qualitative difference with the NCOP case, is that now the condensate also is of thermal origin because the Bragg peak is formed by $\vec{\zeta_{<}}$. Hence, the temperature is not an irrelevant variable. Furthermore, the thermal fluctuations $\vec{\zeta_{>}}$ which obey standard scaling, as the time goes on propagate from the large wave vectors toward the small wave vectors, following a pattern which is important, as we shall see below, for understanding what happens in the realistic systems. Finally, the $\vec{\sigma}$ contribution which was responsible for the condensate with NCOP, here is subdominant, but it can give rise to interesting preasymptotic behaviors if Δ and T_F are appropriately chosen.

In the numerical study of the structure factor, we shall devote particular attention to the transition from preasymptotic to asymptotic features. This we do both for NCOP and COP with d = 3 and d = 2. Parameters of the quench are the final temperature T_F and the strength Δ of the fluctuations in the initial state (15). In particular, we will consider the two cases $\Delta = 0$ (small Δ) and $\Delta = -r/g$ (large Δ), where $\sqrt{-r/g}$ is the equilibrium value of the order parameter at zero temperature. The final temperature of the quench is important in two respects. First of all, for $T_F > T_c$ the correlation length ξ is finite, while for $T_F \leq T_c$ it is infinite. This is important because the general structure of the time evolution is determined by the relation between a microscopic length L_0 and the correlation length ξ in the final equilibrium state. The initial fast transient, with no scaling, lasts up to some time t_0 . At this point equilibrium is established over the length scale L_0 and, if this is of the order of magnitude of ξ , final equilibrium is reached over the whole system as well. Instead, if $\xi \gg L_0$, a second regime is entered [17], during which the scaling relations (1) and (2) hold. This lasts up to the time t_1 such that $L(t_1) \simeq \xi$, when global equilibrium is again established. Clearly, if ξ is infinite, equilibrium is never reached and the scaling regime lasts forever. The second important feature involving the final temperature is that, while for $T_F \geq T_c$ only the thermal fluctuations grow, for $T_F < T_c$ there is growth of both the condensate and thermal fluctuations.

A. Multiscaling analysis

The interplay of all these elements produces a rich variety of behaviors which can be efficiently monitored through the multiscaling analysis. This works as follows: let us assume that the structure factor can be written in the general multiscaling form

$$C(\vec{k},t) = [\mathcal{L}_1(t)]^{\alpha(x)} F(x) \tag{56}$$

with $x = k\mathcal{L}_2(t)$ and where $\mathcal{L}_1(t)$ and $\mathcal{L}_2(t)$ are two lengths. The functions $\alpha(x)$ and F(x) are to be determined. In order to check on the assumption, the time axis is divided in intervals $(t_i, t_i + \tau_i)$ which in practice may also be of variable length τ_i , and within each interval the logarithm of $C(\vec{k}, t)$ is plotted against the logarithm of $\mathcal{L}_1(t)$ for a fixed value of x. By measuring the slope and the intercept of the plot $\alpha(x, t_i)$ and $F(x, t_i)$ are obtained. The procedure is then repeated for different values of x and over different time intervals. If $\alpha(x, t_i)$ and $F(x, t_i)$ do not depend on t_i the assumption (56) is correct and scaling holds. Specifically, standard scaling is the case where $\mathcal{L}_1(t) = \mathcal{L}_2(t)$ and $\alpha(x)$ does not depend on x. In the case of multiscaling $\alpha(x)$ does depend on x and the two lengths $\mathcal{L}_1(t)$ and $\mathcal{L}_2(t)$ differ by a logarithmic factor. Conversely, if $\alpha(x, t_i)$ and $F(x, t_i)$ do depend on t_i , scaling does not hold. Notice that in the case that equilibrium has been reached, the disappearance of the time dependence shows up as $\alpha(x, t_i) \equiv 0$. In the following we shall not be interested in the determination of F(x) and we shall concentrate on $\alpha(x)$.

As an example, consider the quench to $T_F = 0$. With NCOP the exact form of the structure factor is given by [8]

$$C(\vec{k},t) = \Delta \exp\left\{-[Q(t) + (kL)^2]\right\}$$
(57)

where Q(t) is a function of time and $L(t) = t^{1/2}$. Hence, we have the natural choice $\mathcal{L}_2(t) = L(t)$ and, using (56),

$$\alpha(x,t) = -\frac{Q(t)}{\log \mathcal{L}_1(t)} \tag{58}$$

which shows that if there is scaling it is of the standard type. This occurs for large time where $Q(t) = -d \log L(t)$ suggests to take $\mathcal{L}_1(t) = \mathcal{L}_2(t) = L(t)$, yielding $\alpha(x,t) = d$. Conversely, for short time, if Δ is small enough to allow for the application of the linear approximation, we have Q(t) = 2rt and there is no scaling since the time dependence does not drop out

$$\alpha(x,t) = -\frac{2rt}{\log L(t)}.$$
(59)

With COP, instead, the exact form of the structure factor is given by [8]

$$C(\vec{k},t) = \Delta \exp\left(k_m L\right)^4 \psi(k/k_m) \tag{60}$$

where $k_m(t)$ is the peak wave vector, $L(t) = t^{1/4}$ and ψ is given by (9). Choosing $\mathcal{L}_2(t) = k_m^{-1}(t)$ we find

$$\alpha(x,t) = \frac{\left[k_m(t)L(t)\right]^4 \psi(x)}{\log \mathcal{L}_1(t)} \tag{61}$$

which shows that the x dependence cannot be eliminated and therefore that scaling can only be of the multiscaling type. This occurs for large time with $\mathcal{L}_1(t) = \left(k_m^{2-d}L^2\right)^{1/d}$ yielding

$$\alpha(x,t) = d\psi(x). \tag{62}$$

Using (11), the two lengths $\mathcal{L}_1(t)$ and $\mathcal{L}_2(t)$ are related by $\frac{\mathcal{L}_1(t)}{\mathcal{L}_2(t)} \sim (\log L)^{2/d}$. Conversely, in the very early stage where the linear approximation holds $\mathcal{L}_2(t) = k_m^{-1} = \sqrt{-2/r}$ is time independent and $\mathcal{L}_1 \sim t^{1/2d}$ yielding

$$\alpha(x,t) \sim \frac{t}{\log t} \psi(x) \tag{63}$$

which displays the absence of scaling through a time dependent prefactor in front of $\psi(x)$.

B. Evolution of $\alpha(x,t)$

In the following we illustrate the evolution of $\alpha(x,t)$ obtained numerically over a sequence of time intervals, with r = -1 and g = 1.

NCOP d = 3

Let us begin with NCOP in the three dimensions. The critical temperature is finite $T_c = 2\pi$, the exponent α is obtained setting $\mathcal{L}_1(t) = \mathcal{L}_2(t)$ and extracting this length from the inverse of the halfwidth of the structure factor. According to the general outline presented at the beginning of this section, we expect to detect the establishment of equilibrium for $T_F > T_c$ through the vanishing of α and the scaling behavior lasting indefinitely for $T_F \leq T_c$, through the disappearance of the time dependence around a non vanishing value of α . This is clearly illustrated in Fig. 3, where α is plotted for a quench well above T_c with $T_F = 20$ and for a quench to T_c . In the first case the lines rapidly collapse on $\alpha = 0$, while in the second case the collapse is on $\alpha = 2$. It is then interesting to consider the case of a final temperature slightly above T_c , which corresponds to a large but finite ξ . Also in this case α is expected to collapse eventually on $\alpha = 0$, however as long as L(t) is large but smaller than ξ , one expects to observe a behavior similar to the one in the quench to T_c . Indeed, this is what happens in Fig. 4 (panel a), obtained by plotting α for $T_F = 6.35$. After the initial transient there is a collapse on $\alpha = 2$, revealing critical scaling. However, this does not last indefinitely as in the case of the quench to T_c , but it lasts for the time necessary for L(t) to catch up with ξ . After this a new transient sets in and the eventual collapse on the equilibrium value $\alpha = 0$ takes place. For $T_F < T_c$ the behavior of α is quite similar to the one for $T_F = T_c$, since in both cases $\xi = \infty$. The only difference is that the asymptotic behavior produces collapse on the value $\alpha = d = 3$. For T_F slightly below T_c , e.g $T_F = 6.20$ in Fig. 4 (panel b), there is crossover from critical scaling with $\alpha = 2$ to the final value with $\alpha = 3$. In general, the asymptotic behavior for $0 < T_F < T_c$ and $T_F = 0$ is the same (Fig. 5), confirming the irrelevance of thermal fluctuations. In all quenches considered, the variation of the size Δ of initial fluctuations does not produce significant differences.

NCOP
$$d = 2$$

In two dimensions the critical temperature (26) vanishes. So, for any $T_F > 0$ one should observe a behavior for α similar to the one obtained with d = 3 and $T_F > T_c$. This is the case for quenches with a final temperature well above zero, where behaviors of α very close to the one in panel a of Fig. 3 are obtained. Similarly, for the quench to $T_F = 0$ the same behavior of Fig. 5 (panel b) is obtained, except that now the lines collapse on $\alpha = d = 2$.

A case to be considered separately is when T_F is finite but very close to zero. Fig. 6 corresponding to $T_F = 0.3$ and $T_F = 10^{-6}$, displays an intermediate scaling behavior with $\alpha = 2$ preceding the eventual collapse on the equilibrium value $\alpha = 0$. At first sight this looks like the behavior of Fig. 4 (panel *a*) in the quench to a final temperature slightly above T_c . However, the interpretation is more subtle, since what is growing here, as long as $L(t) < \xi$, are not the critical fluctuations but the condensate. The distinction between condensation and critical behavior is actually impossible to make with NCOP on the basis of the value of α , since with d = 2 in both cases $\alpha = 2$. This remark will become clear with COP, because in that case the growth of the critical fluctuations is associated to standard scaling, while the growth of the condensate gives rise to multiscaling.

COP d = 3

We now move on to the case of COP with both small and large initial fluctuations. As discussed above, $\alpha(x,t)$ is extracted by defining $x = k/k_m$, where $k_m(t)$ is the peak wave vector, and plotting $\log C$ vs. $\log \mathcal{L}_1(t)$ with $\mathcal{L}_1(t) = (k_m^{2-d}L^2)^{1/d}$ and $L(t) = t^{1/4}$. For quenches to $T_F \geq T_c$ the behavior of $\alpha(x,t)$ essentially follows the same pattern as in the NCOP case. Apart from some differences in the time dependent transients, again for $T_F > T_c$ and for $T_F = T_c$ curves collapse, respectively, on $\alpha = 0$ and $\alpha = 2$. In Fig. 7 we illustrate what happens in the quench slightly above (panel a) and slightly below (panel b) T_c . In both cases there is a preasymptotic standard scaling behavior with $\alpha = 2$ due to the critical point in the neighborhood, followed by the incipient crossover toward the asymptotic behavior. Above T_c this is $\alpha = 0$, as revealed by α deviating downward, while below T_c the deviation occurs upwardly, for $x < x^*$, toward the asymptotic form of Fig. 1.

Where the difference between NCOP and COP becomes remarkably evident is in the quenches well below T_c . Let us first consider (Fig. 8) $T_F = 0$. After a time dependent transient (panel a), which for small Δ in the early stage is well described by (63), the curves of $\alpha(x, t)$ collapse (panel b) on the limiting curve (62) depicted in Fig. 1. Instead, for $T_F = 1$ (Fig. 9), the collapse occurs on the finite temperature asymptotic form of Fig. 1, with minor differences in the transient due to the size of Δ . However, going to a temperature much lower but finite (Fig. 10), while for $\Delta = 0$ (panel a) α follows the same pattern as in Fig. 9, the behavior in panel b with $\Delta = 1$ is drastically different. What we have here is multiscaling as in the quench to $T_F = 0$, for $x < x^*$, and standard scaling with $\alpha = 2$ for $x > x^*$. All these features can be accounted for on the basis of the discussion made at the beginning of this section. As long as T_F is sufficiently large or Δ small, as in Fig. 9 and in panel a of Fig. 10, only $C_{<}(\vec{k}, t)$ and $C_{>}(\vec{k}, t)$ contribute to $\alpha(x, t)$ producing the characteristic behavior of Fig. 1. However, when Δ is finite and T_F small enough, there can be a sizable interval of time during which $C_0(\vec{k}, t)$ dominates over $C_{<}(\vec{k}, t)$, for $x < x^*$, producing the scaling pattern of panel b in Fig. 10. This behavior is preasymptotic and eventually the crossover to the pattern of Fig. 9 takes place, as $C_{<}(\vec{k}, t)$ grows large enough to overtake $C_0(\vec{k}, t)$. In our numerical solution the computation was not run long enough to actually detect this crossover, but it is clear that by modulating the parameters of the quench, Δ and T_F , the crossover time can be varied at will.

COP d = 2

It is now interesting to see how this variety of behaviors is affected by pushing the critical temperature to zero in two dimensions. The novelty with respect to the previous case is that now the line of fixed points in between $T_F = 0$ and T_c has disappeared and with it, supposedly, also the associated asymptotic behavior. Actually, only the fixed point at $T_F = 0$ has survived. Thus we should observe either the relaxation to equilibrium for $T_F > 0$, or the multiscaling behavior for $T_F = 0$. Indeed, for temperatures like $T_F = 10$ the collapse on $\alpha = 0$ is observed. Similarly, the quench to $T_F = 0$ produces a behavior identical to the one in Fig. 8, except that the peak value of α is given by 2 in place of 3. The interesting novelties arise when quenches to small, but finite, T_F are considered. In fact, when T_F is low ξ is large and an intermediate scaling regime preceding the final equilibration is expected. The question is, what it will be like. For $T_F = 10^{-6}$ (Fig. 11) and $\Delta = 0$ there is standard scaling with $\alpha = 2$, while for $\Delta = 1$ the pattern is identical to the one in panel b of Fig. 10, except for the obvious modification $\alpha(x = 1) = d = 2$. The first observation is that these are preasymptotic behaviors, since eventually α must vanish. The second is that this phenomenology can be understood regarding, as long as $L(t) < \xi$, the structure factor as made up of the three contributions (52-54). Namely, as long as $L(t) < \xi$, there is growth of the condensate and of thermal fluctuations, as in the quench below the critical point. Thermal fluctuations are clearly due to $T_F > 0$, while the growth of the condensate originates from the underlying fixed point being at $T_F = 0$. The net result is that the intermediate scaling behavior with $\Delta = 0$ is due to

 $C_{\leq}(\vec{k},t)$ and $C_{\geq}(\vec{k},t)$, which scale both like L^2 since ρ vanishes when d = 2. Instead, with $\Delta = 1$ we are confronted again with a situation where, in the time of the computation, $C_0(\vec{k},t)$ dominates over $C_{\leq}(\vec{k},t)$ producing the pattern of panel b. As a matter of fact this is a pre-preasymptotic scaling behavior, since when $C_{\leq}(\vec{k},t)$ overtakes $C_0(\vec{k},t)$ a behavior of the type in panel a is expected to occur before the eventual relaxation to a vanishing α .

IV. CONCLUSIONS

In this paper we have investigated the origin of the non commutativity of the limits $t \to \infty$ and $N \to \infty$ in the dynamics of the first order transitions. The main result is that when the $N \to \infty$ limit is taken first the underlying phase transition, which we have called condensation, is qualitatively different from the usual process of ordering obtained with the limits in the opposite order. In particular, condensation in conjunction with COP gives rise, for reasons which are not yet clear, to two phenomena which are strikingly different from what one has in phase-ordering, namely i) multiscaling and ii) relevance of the thermal fluctuations. We have then proceeded to an extensive investigation of the scaling properties of the structure factor in the large-N model for quenches to a final temperature greater, equal or lower than T_c . We have found a rich variety of behaviors, which can be studied in great detail through the multiscaling analysis. Particularly interesting is the existence of preasymptotic scaling which can be explained through the competition between different components of the order parameter with distinct scaling properties.

Even though it is quite clear that the large-N model is not perturbatively close to the phase-ordering processes in realistic systems, in concluding the paper we wish to elaborate on the connections that nonetheless exist. In order to do this we use the BH model [11] as an intermediate step. As mentioned above, in this model the structure factor for the quenches to $T_F = 0$ with COP displays standard scaling for any finite value of N. The discussion in the previous section on the behavior of α in the quenches to $T_F = 10^{-6}$ helps to understand how this comes about. By integrating formally the equation of motion, the BH structure factor can be written as the sum of two contributions

$$C(\vec{k},t) = C_0(\vec{k},t) + C_N(\vec{k},t)$$
(64)

where $C_0(\vec{k}, t)$ is given by (44) while

$$C_N(\vec{k},t) = -\frac{2}{N}k^p \int_0^t dt' R(t') \frac{C_0(\vec{k},t)}{C_0(\vec{k},t')} D(\vec{k},t')$$
(65)

with

$$D(\vec{k},t) = \int \frac{d^d k_1}{(2\pi)^d} \frac{d^d k_2}{(2\pi)^d} C(\vec{k} - \vec{k}_1, t) C(\vec{k}_1 - \vec{k}_2, t) C(\vec{k}_2, t)$$
(66)

contains the nonlinearity and R(t) is given by (28) and (29). Although Eq. (43) refers to a quench to $T_F > 0$ with $N = \infty$ and Eq. (64) to a quench to $T_F = 0$ and N finite, the mechanism regulating the competiton between the two terms is the same. In particular, in both cases $C_0(\vec{k},t)$ can compete with the second term only for $x < x^*$. BH have shown that $C_N(\vec{k},t)$ asymptotically obeys standard scaling with $\alpha = d$. It is then clear that by choosing Δ and N properly there may be a preasymptotic regime during which $C_0(\vec{k},t)$ dominates for $x < x^*$, much in the same way as in the previous section $C_0(\vec{k},t)$ was found to dominate over $C_T(\vec{k},t)$. Here 1/N plays a role similar to that of T_F and the crossover time depends on both Δ and N [11,14]. With N = 100 and d = 2 (Fig. 12) a behavior for $\alpha(x,t)$ is obtained which is practically the same of that in Fig. 11. In order to complete the picture, we reproduce in Fig. 13 the behavior of $\alpha(x,t)$ for the scalar system obtained in Ref. [15] by the simulation of Eq. (12) with N=1 and d=2. Again the same pattern is found, revealing that the same mechanism is operating also in this case. Therefore, one may conclude that the behavior of the large-N model associated to $C_0(\vec{k},t)$ describes what happens in the preasymptotic regime also in the phase-ordering processes over the shrinking range of wave vectors with $k < x^* k_m(t)$. In other words, the asymptotic regime is preceded by a time regime where phase-ordering over the short length scale seems to coexist with condensation over the large length scale. This is not surprising for NCOP since correlations are established over regions of size L(t), and the statistics can be expected to become gaussian over distances larger than L(t). For COP it is less straightforward, although the occurrence of gaussian statistics on large length scales can be detected much more easily through the appearence of multiscaling behavior.

V. APPENDIX I

From (1) the real space scaling form of the correlation function is given by

$$G(\vec{r},t) = r^{\alpha-d}g(r/L(t)) \tag{67}$$

where g(x) is the scaling function and g(0) is a finite quantity. For $r \ll L(t)$ (67) gives the equilibrium decay of the correlation function

$$G_{ea}(\vec{r}) \sim r^{\alpha - d}.\tag{68}$$

On the other hand, the correlation function on a fractal [18], decays as

$$G_{eq}(\vec{r}) \sim r^{2(D-d)} \tag{69}$$

where D is the fractal dimensionality. Comparing (69) with (68) the fractal dimensionality of the correlated regions is given by $D = \frac{1}{2}(\alpha + d)$ and using (3)

$$D = \begin{cases} \frac{1}{2}(2+d-\eta), & \text{for } T_F = T_c \\ d, & \text{for } T_F < T_c. \end{cases}$$
(70)

VI. APPENDIX II

NCOP

Equation (37) can be rewritten as

$$\xi^{-2} = r + gT_F B(0) + \frac{gT_F}{V\xi^{-2}} + gT_F \left[B(\xi^{-2}) - B(0) \right]$$
(71)

and using $r + gT_cB(0) = 0$

$$\frac{\xi^{-2}}{g} = c + T_F \left[B(\xi^{-2}) - B(0) \right]$$
(72)

where

$$c = -\frac{r}{g} \left(\frac{T_F - T_c}{T_c} \right) + \frac{T_F}{V\xi^{-2}}.$$
(73)

Since $[B(\xi^{-2}) - B(0)]$ is a non positive monotonously decreasing function, there is a positive solution of (72) for c > 0, a vanishing solution for c = 0 and no solution for c < 0. For $T_F < T_c$ the quantity c cannot be positive, because in that case ξ^{-2} would be positive and the second term in the right hand side of (73) would vanish in the infinite volume limit, producing c < 0. Therefore, c can only vanish implying

$$\lim_{V \to \infty} \frac{T_F}{V\xi^{-2}} = \gamma^2 = -\frac{r}{g} \left(\frac{T_c - T_F}{T_c}\right).$$
(74)

COP

With conserved order parameter, Eq. (36) is replaced by

$$\xi^{-2} = r + \frac{gT_F}{V} \sum_{\vec{k} \neq 0} \frac{1}{k^2 + \xi^{-2}}$$
(75)

which allows for a solution $\xi^{-2} > -k_{min}^2$, where $k_{min} \sim V^{-1/d}$ is the minimum value of the wave vector. For

$$T_F < \tilde{T}_c = -\frac{r}{g} \left[\frac{1}{V} \sum_{\vec{k} \neq 0} \frac{1}{k^2} \right]^{-1}$$
(76)

the solution is negative $-k_{min}^2 < \xi^{-2} < 0$. In the infinite volume limit $\tilde{T}_c \to T_c$ and $\xi^{-2} \to -k_{min}^2$. Thus, rewriting (75) as

$$\xi^{-2} = r + gT_F B(\xi^{-2}) + \frac{gT_F}{V(k_{min}^2 + \xi^{-2})}$$
(77)

we can analyze this equation exactly as in the NCOP case, obtaining for $T_F < T_c$ the analog of (74)

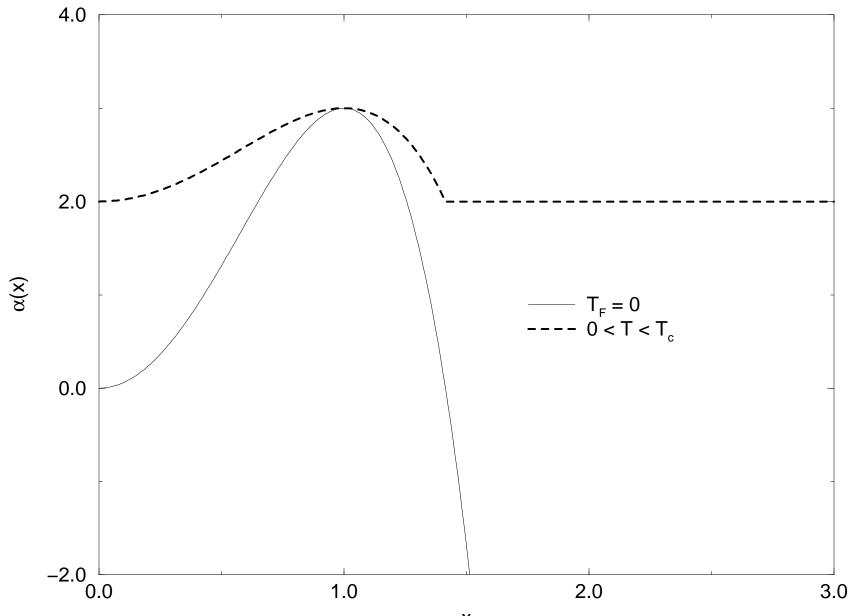
$$\lim_{V \to \infty} \frac{T_F}{V(k_{min}^2 + \xi^{-2})} = \gamma^2 = -\frac{r}{g} \left(\frac{T_c - T_F}{T_c}\right).$$
(78)

- [1] For a review, see A. J. Bray, Adv. Phys. 43, 357 (1994).
- [2] The formal structure for this program can be found in G. F. Mazenko, O. T. Valls and M. Zannetti, Phys. Rev. B 38, 520 (1988).
- [3] H. K. Janssen, B. Schaub and B. Schmitt, Z. Phys. B 73, 539 (1989); H. K. Janssen, On the renormalized field theory of nonlinear critical relaxation in From phase transitions to chaos p.68, G. Gyorgyi, I. Kondor, L. Sasvari and T. Tèl editors, World Scientific (1992).
- [4] J. W. Cahn and J. E. Hilliard, J. Chem. Phys. 31, 688 (1959).
- [5] T. Ohta, D. Jasnow and K. Kawasaki, Phys. Rev. Lett. 49, 1223 (1982); G. F. Mazenko, Phys. Rev. B 42, 4487 (1990);
 43, 5747 (1991). The gaussian auxiliary field approximations are critically reviewed in C.Yeung, Y.Oono and A.Shinozaki, Phys. Rev. E 49, 2693 (1994).
- [6] K.R.Elder, T.M.Rogers and R.C.Desai, Phys. Rev. B 38, 4725 (1988); J.S.Langer, An introduction to the kinetics of first order transitions in Solids far from equilibrium, Ed. C. Godrèche, Cambridge Univ. Press (1992).
- [7] A.J.Bray and K.Humayun, Phys. Rev. E 48, R1609 (1993); S.De Siena and M.Zannetti, Phys. Rev. E 50, 2621 (1994);
 G.F.Mazenko, Phys. Rev. E 49, 3717 (1994); 50, 3485 (1994).
- [8] A.Coniglio and M.Zannetti, Europhys. Lett 10, 575 (1989).
- [9] G.F.Mazenko and M.Zannetti, Phys. Rev. B 32, 4565 (1985)
- [10] A.Coniglio, P.Ruggiero and M.Zannetti, Phys. Rev. E 50, 1046 (1994).
- [11] A.J.Bray and K.Humayun, Phys. Rev. Lett. 68, 1559 (1992).
- [12] T.H.Berlin and M.Kac, Phys. Rev. 86, 821 (1952).
- [13] H.W.Lewis and G.H.Wannier, Phys. Rev. 88, 682 (1952); 90, 1131E (1953).
- [14] C.Castellano and M.Zannetti, Phys. Rev. E 53, 1430 (1996).
- [15] C.Castellano and M.Zannetti, Phys. Rev. Lett. 77, 2742 (1996).
- [16] For a comparative discussion of the two models see M.Kac and C.J.Thompson, J. Math. Phys. 18, 1650 (1977).
- [17] G.F.Mazenko, Phys. Rev. B 26, 5103 (1982).
- [18] T.Vicsek, Fractal Growth Phenomena, World Scientific 1989.

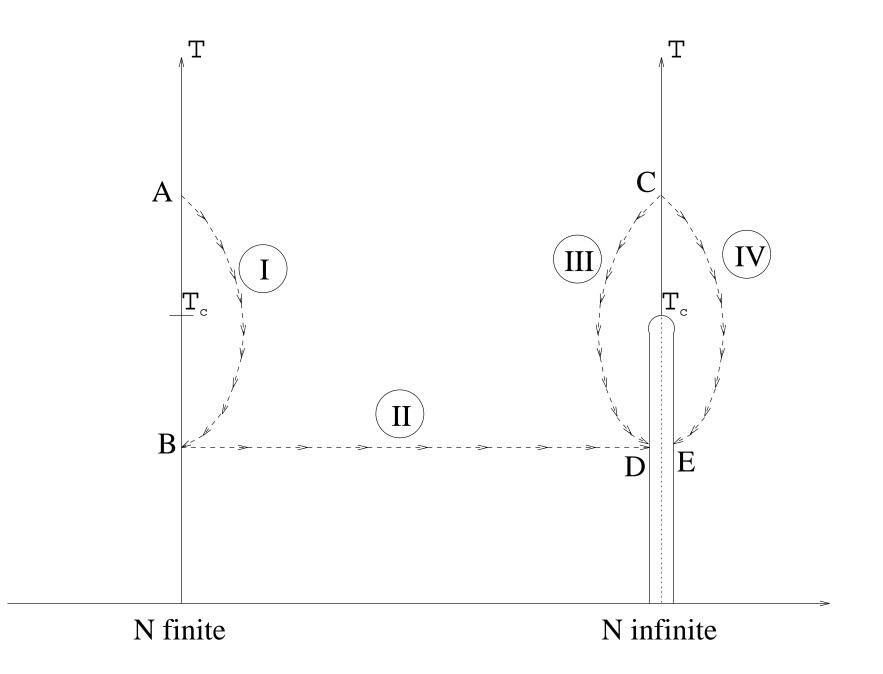
FIGURE CAPTIONS

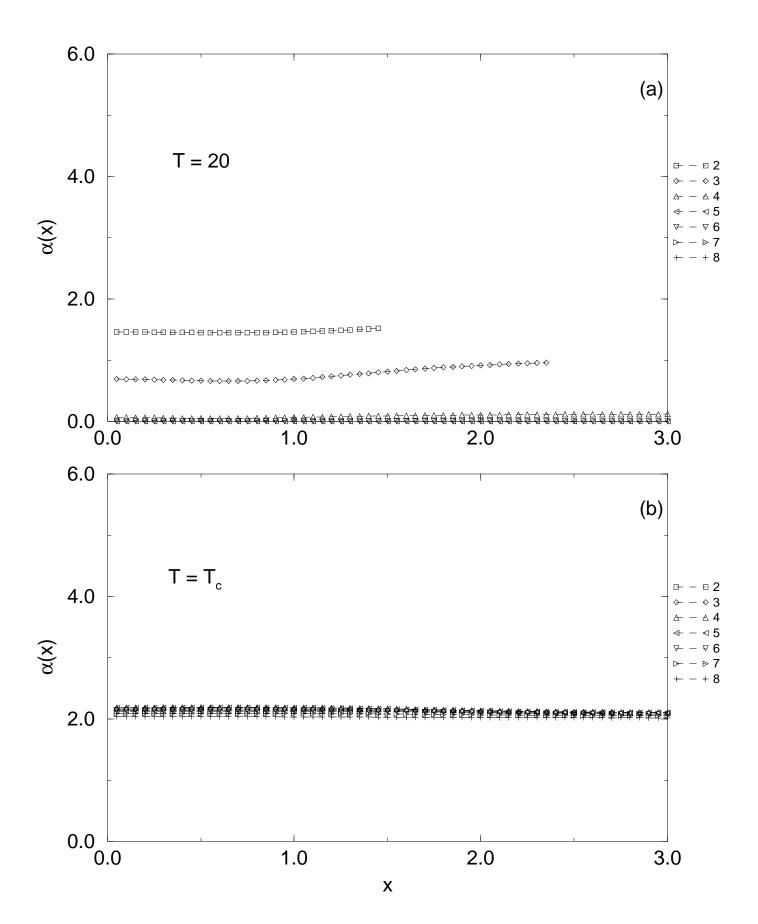
- 1. Spectrum of the multiscaling exponent $\alpha(x)$ for quenches with COP and d = 3.
- 2. Schematic representation of the relaxation processes in the systems with N finite and $N = \infty$.
- 3. Evolution of $\alpha(x)$ for NCOP, d = 3. (a) $T_F \gg T_c$ (b) $T_F = T_c$. Different curves refer to a sequence of time intervals growing exponentially with the label. In this and all other figures except Fig. 8, very early times are not shown for simplicity.
- 4. Evolution of $\alpha(x)$ for NCOP, d = 3 for quenches to T_F slightly above and slightly below T_c . Symbols and time intervals are related as in Fig. 3.
- 5. Evolution of $\alpha(x)$ for NCOP, d = 3 for quenches to $0 < T_F < T_c$ and $T_F = 0$. Symbols and time intervals are related as in Fig. 3.
- 6. Evolution of $\alpha(x)$ for NCOP, d = 2 for quenches to $T_F = 0.3$ and $T_F = 10^{-6}$. Symbols and time intervals are related as in Fig. 3.
- 7. Evolution of $\alpha(x)$ for COP, d = 3 for quenches to T_F slightly above and slightly below T_c . Symbols and time intervals are related as in Fig. 3.
- 8. Evolution of $\alpha(x)$ for COP, d = 3 for a quench to $T_F = 0$. (a) early times (b) intermediate to late times. Different curves refer to a sequence of time intervals growing exponentially with the label.
- 9. Evolution of $\alpha(x)$ for COP, d = 3, $T_F = 1$. (a) zero initial fluctuations, (b) large initial fluctuations. Symbols and time intervals are related as in Fig. 3.
- 10. Evolution of $\alpha(x)$ for COP, d = 3, $T_F = 10^{-6}$. (a) zero initial fluctuations, (b) large initial fluctuations. Symbols and time intervals are related as in Fig. 3.

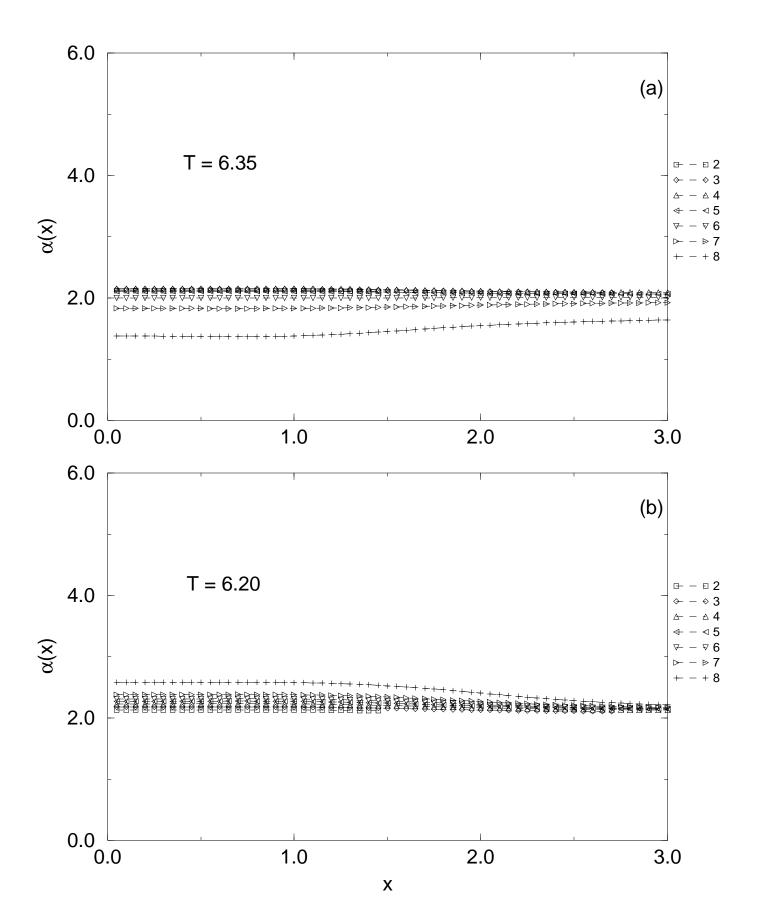
- 11. Evolution of $\alpha(x)$ for COP, d = 2, $T_F = 10^{-6}$. (a) zero initial fluctuations, (b) large initial fluctuations. Symbols and time intervals are related as in Fig. 3.
- 12. Evolution of $\alpha(x)$ for the solution of the Bray-Humayun model with N = 100, d = 2, $T_F = 0$. (a) small initial fluctuations, (b) large initial fluctuations. Different curves refer to a sequence of time intervals growing exponentially with the label.
- 13. Evolution of $\alpha(x)$ obtained in Ref. [14] by simulation of a system with N = 1, d = 2 and $T_F = 0$. (a) small initial fluctuations, (b) large initial fluctuations. Different curves refer to a sequence of time intervals growing exponentially with the label.

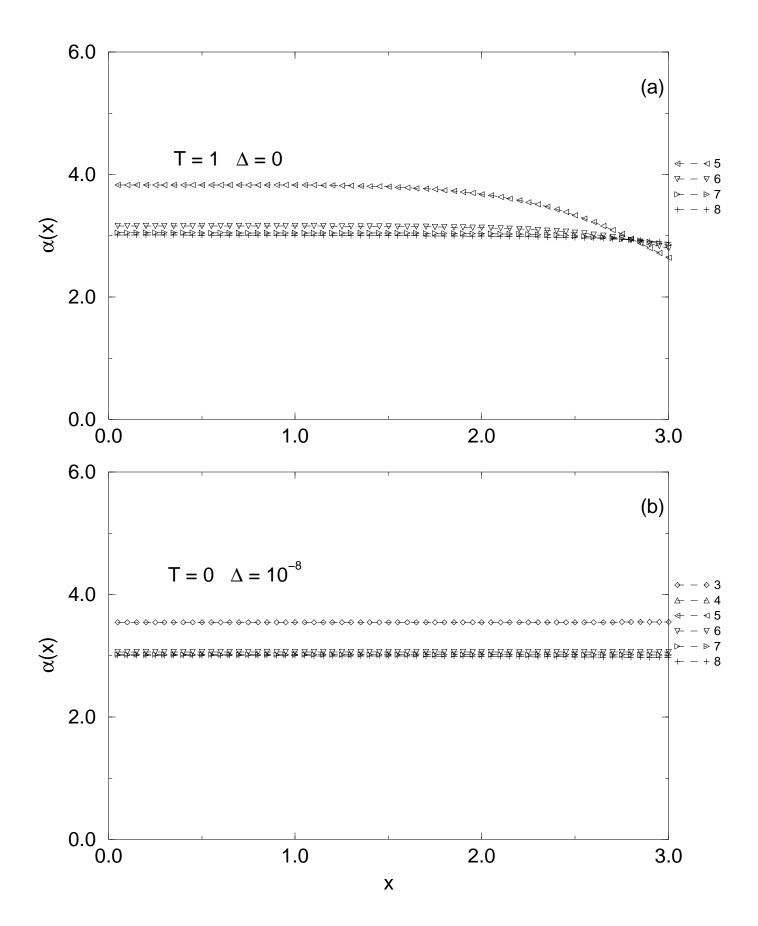


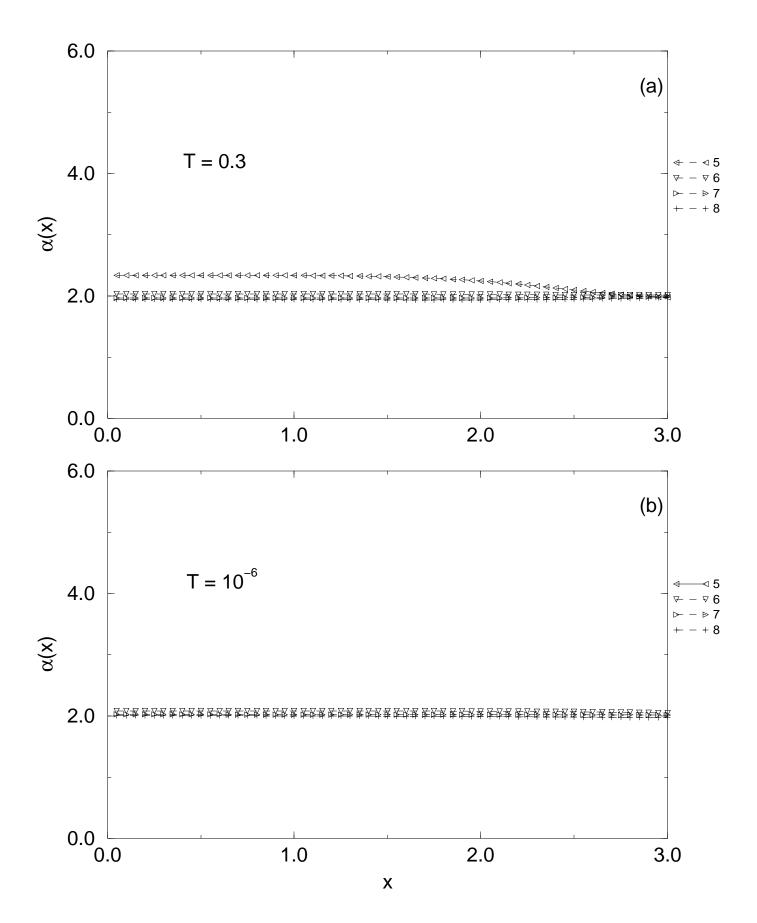
Х

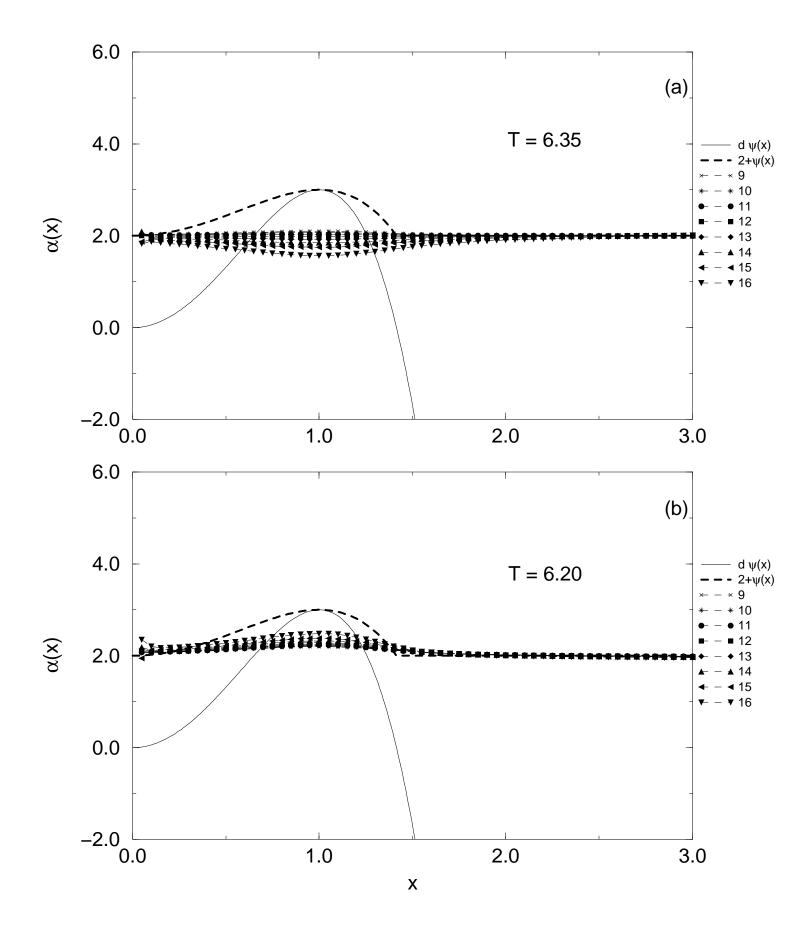


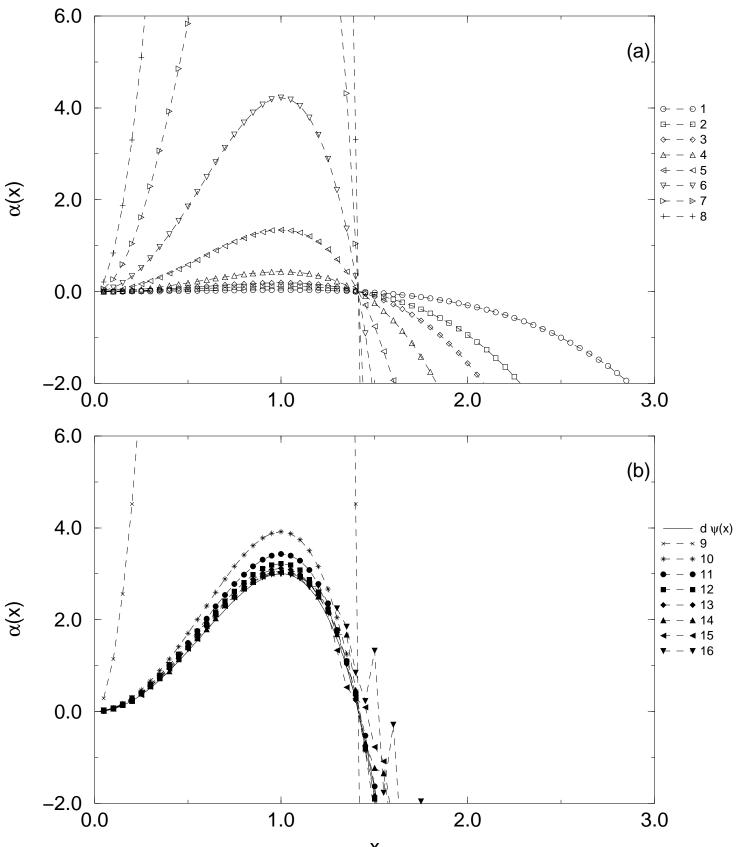












Х

